THIS MATERIAL WAS TAKEN FROM THE PH.D. THESIS OF KAY A. SANDBERG, DEPARTMENT OF CHEMISTRY, NC STATE UNIVERSITY, 1998

IX.1 Spin-Spin Interactions

We have examined the energy expression describing the exchange interaction of electrons 1 and 2 for a diradical system according to the isotropic Heisenberg Hamiltonian $\hat{H} = -2J\hat{S}_1\hat{S}_2$ where the eigenfunctions are the singlet and triplet functions and the eigenvalues are separated by $2J$[1] as shown in Figure IX.1. For an exchange-coupled diradical system the spin-spin interaction for the populated triplet state is detectable by EPR. As previously described in Section VIII.2.1 the hyperfine coupling constant when $J >$ a is half that of the monoradical. Another spin-spin interaction that is generally detectable by EPR is described by the zero field splitting (ZFS) parameters ***D*** and ***E*** and is also shown in Figure IX.1. The energy of this interaction is given by the spin-spin Hamiltonian $\hat{H} = \hat{S} \cdot \mathbf{D} \cdot \hat{S}$ and describes the energy separation within the triplet manifold. The exchange and dipolar interactions then are the interactions which lift the degeneracy of the four spin states (the one singlet state and the three substates of the triplet state) where the exchange interaction lifts the degeneracy between the singlet and triplet states and the dipolar interaction lifts the degeneracy of the three triplet substates. Before discussing the theoretical aspects of the ZFS parameters for a diradical, we present the physical manifestations of ***D*** and ***E*** via EPR.

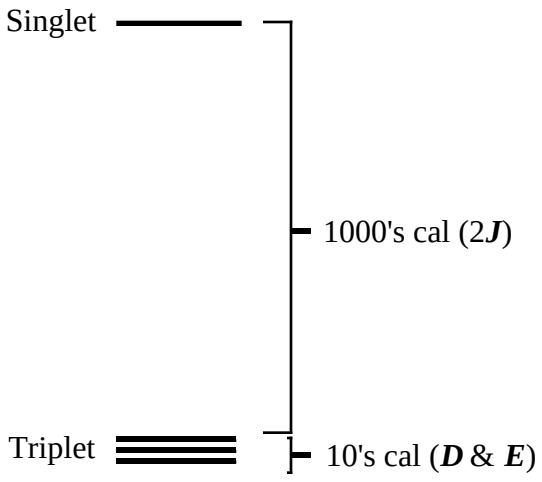

Figure IX.1. Introductory description of ***J*** , ***D*** and ***E***.

IX.2 The EPR Experiment[2]

Systems with $S > 0$ will experience a quantization of spin states when placed in an applied magnetic field and exhibit discrete spin states according to the multiplicity rule $2S + 1$. Thus for a system with one

unpaired electron (S = 1/2), the multiplicity is a doublet [2(1/2) + 1 = 2], i. e., there are two spin states, α and β, with spin quantum numbers (M_S) equal to +1/2 and -1/2, respectively. The interaction between the spin and the field is described by the Zeeman effect — the energy separation of the two spin states increases with the increase of the applied magnetic field according to the expression

$$E = g\beta M_S H \tag{1}$$

where g is the electronic g-factor, β is the Bohr magneton, M_S is the spin quantum number and H is the applied field. In the absence of an applied field the α or β spin states of the electron are degenerate as shown in Figure IX.2. Application of an applied field lifts the degeneracy of the two spin states. The α spin state, whose magnetic moment opposes the applied field, rises in energy while the β spin state, whose magnetic moment is aligned with the applied field, decreases in energy as the strength of the applied field increases. When a frequency of energy which matches the energy separation between the two spin states is applied an absorption occurs which causes a transition between the two spin states. The selection rule $\Delta M_S = \pm 1, \Delta M_I = 0$ governs the transition. (M_I is the nuclear spin quantum number.) This absorption is detected and is the basis of the EPR experiment as shown in Figure IX.2. EPR spectra are usually shown as the first derivative of the absorption curves. The following discussion assumes the EPR experiment is performed by fixing the applied frequency and sweeping the field.

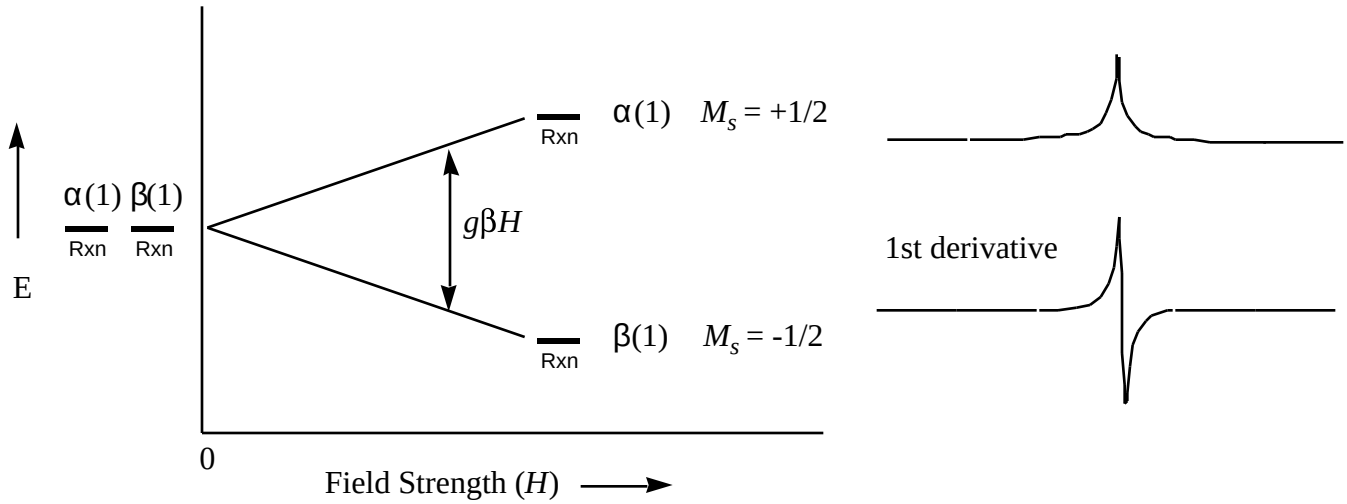

Figure IX.2. Energy diagram and absorption curves for S = 1/2 system.

When two unpaired electrons are present in a system, the state depends upon the alignment of the two electrons as shown in Figure IX.3 and discussed in section II.2. If the unpaired electrons are aligned

antiparallel, the multiplicity is a singlet [2(0) + 1 = 1]. As the name suggests, there is only one spin state and thus no EPR transition is observed. When the spins are aligned parallel (S = 1), the multiplicity is a triplet [2(1) + 1 = 3]. According to the $\Delta M_S = \pm 1$ selection rule, there are two allowed transitions. Figure IX.3 shows the three substates, the allowed transitions and the EPR spectra.

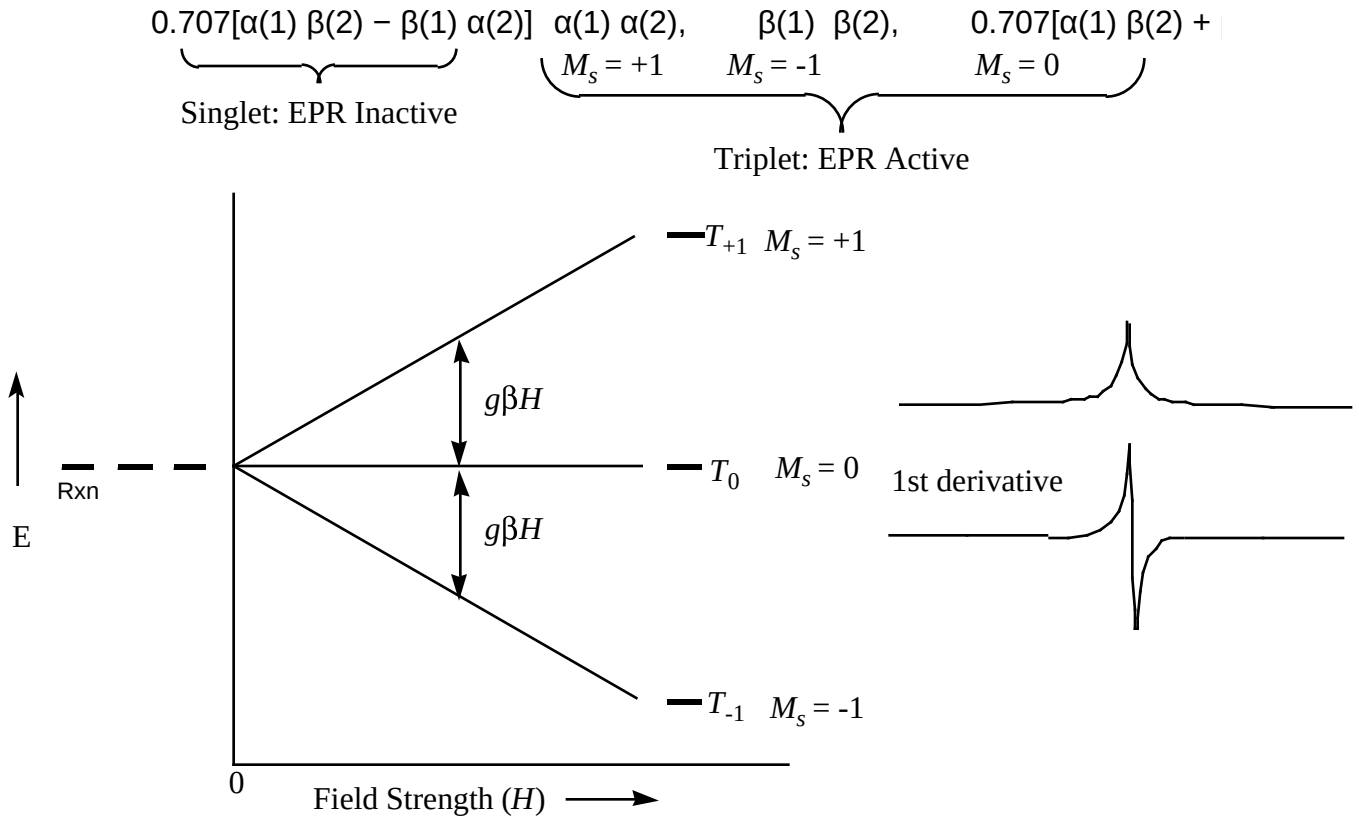

Figure IX.3. Energy diagram and absorption curves for S = 1 system.

Figure IX.3 shows the three sublevels of the triplet state degenerate at zero field. The energy diagram depicts the energy of the electrons as a function of the applied magnetic field only. The effective magnetic field experienced by each electron, however, is the vector sum of several magnetic fields, not just the externally applied field. The internal fields are operative in the absence of the externally applied field and are due to magnetic moments of nuclei, the other unpaired electron and possibly a contribution from each electron's own orbital angular momentum.[3] In the following discussion, however, only the internal magnetic field associated with the spin of the other electron is considered. Two reasons for this simplification are: 1) because the magnetic moment of the electron is approximately three orders of magnitude larger than the nuclear magnetic moment, the influence of its magnetic field is significantly larger than that of the nuclei[4]

and 2) for organic diradicals the orbital contribution is relatively small as evidenced by the relatively small changes in g.[3]

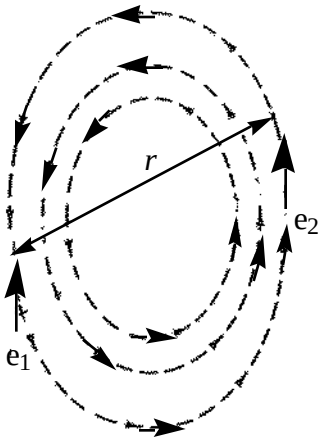

IX.3 The EPR Experiment and the Zero Splitting Parameters *D* and *E*.[5]

To explain the effect of each unpaired electron's magnetic field on the other unpaired electron it is helpful to view the electrons as dipoles that experience repulsive dipole-dipole interaction due to their parallel alignment. As a consequence of this repulsive dipolar coupling the lowest energy state will be the state where the two electrons are furthest apart. Figure IX.4 depicts the energy states of three idealized triplet systems as a function of electron distribution.[5] T_Z represents a state in which the spin axes of the two electrons have been quantized so that they are confined to the XY plane and the component of the spin angular momentum in the Z-direction is zero. Likewise for T_Y the spin axes are confined to the XZ plane with a zero component along the Y-axis and for T_X the spin axes are confined to theYZ plane with a zero component along the X-axis. In (a) the electrons are spherically distributed. There is no direction in which the electrons can move to get further apart to minimize the repulsive dipole-dipole interaction and as a result the three states remain degenerate. In (b) where the spin distribution has been compressed along the Z-axis, the two electrons will experience a more repulsive interaction when they are aligned in either the XZ plane (T_Y state) or YZ plane (T_X state) because they will be closer together. They can stay further apart in the XY plane (T_Z state) which results in a lower energy state. A third scenario adds to the compression along the Z-axis an elongation along the X-axis resulting in the state splitting shown in (c). Again the lowest energy state corresponds to the alignment of the spin axes in the XY plane for the same reason given above. The highest energy states also correspond to the alignment of the spin axes in the planes of Z-direction because of the

major compression along the *Z*-axis, but a further splitting occurs due to the additional elongation along the *X*-direction. The spins experience the largest repulsive interaction (closest proximity) when confined to the *YZ* plane therefore the highest energy state corresponds to alignment of the spin axes in the *YZ* plane (T_X state).

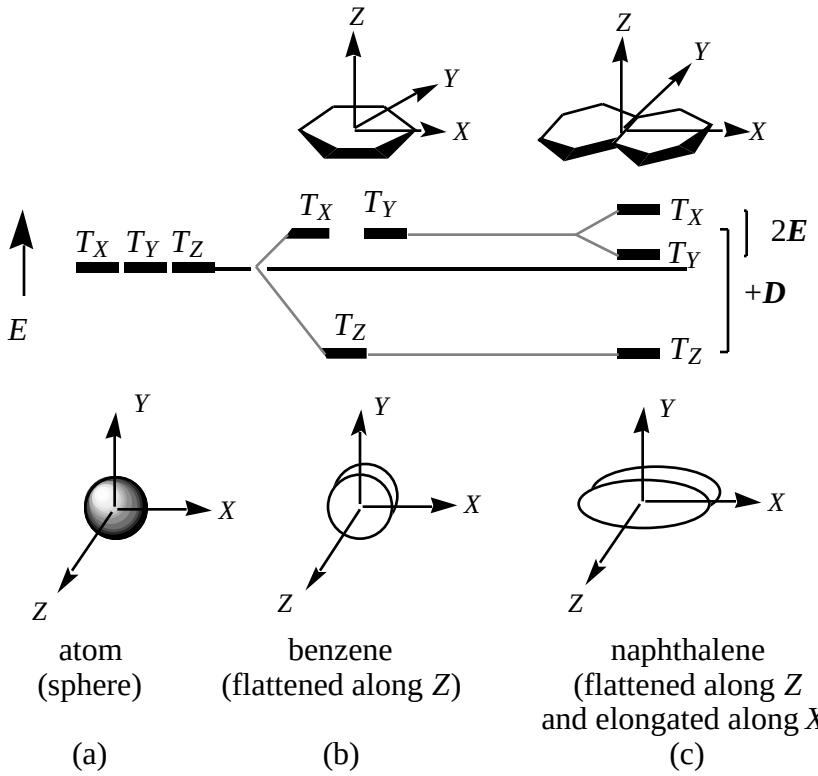

Figure IX.4. Energy states as a function of electron distribution: +***D***.

As described above, the quantization of the spin states does not result from an externally applied field, but rather from the molecular geometry. This energetic effect in zero field is due to the anisotropic electron distribution and is described by the ZFS parameters ***D*** and ***E***. ***D*** is defined as the energy difference between the lower energy state and the higher degenerate energy states as in (b) or between the lowest energy state and the average of the higher two energy states as in (c). The parameter ***E*** is 1/2 the energy difference of the higher energy states. ***D*** is positive for an oblate spin distribution — a flattening in one direction (Figure IX.4). ***D*** can also be negative if the electron distribution is prolate — an elongation in one direction (Figure IX.5). Thus the geometrical shape of the spin distribution can be estimated from ***D*** and ***E***.[6]

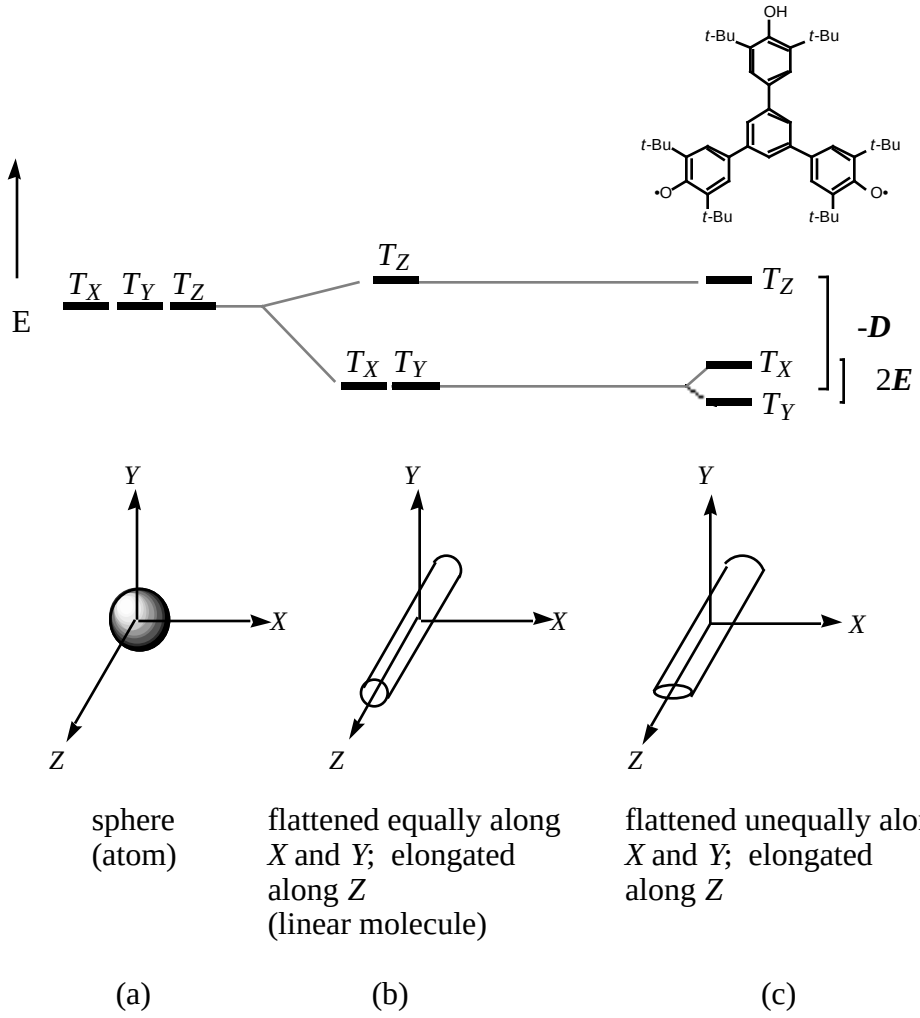

Figure IX.5. Energy states as a function of electron distribution: -***D***.

The two-fold degeneracy in (b) of Figure IX.4 is characteristic of any triplet species which possesses three-fold or higher symmetry and a magnetically isotropic plane perpendicular to the symmetry axis (axial symmetry). The zero field splitting of the energy states of such a triplet is described by ***D***. The zero field splittings of the energy states of a triplet species with lower symmetry (rhombic symmetry) are described by both ***D*** and ***E*** as in (c). For spherical electron distribution (cubic symmetry) as in (a) there is no zero-field energy state splitting. EPR is the technique used to determine the energies of ***D*** and ***E***.

The simplest triplet EPR spectrum is that of a simple atomic triplet system with cubic symmetry. When such a system is placed in an applied magnetic field with the field aligned with the molecular *Z*-axis (H_Z), the electrons whose spin vectors are in the *XY* plane will remain at the same energy (T_0 state) since their spin vectors are perpendicular to the applied field. The electrons whose spin vectors are in either the *XZ* or *YZ* planes however will either be stabilized or destabilized depending on whether the magnetic moments are

aligned with (T_{-1} state) or against (T_{+1} state) the applied field, respectively. As shown in Figure IX.6 there are two allowed transitions, but since they occur at the same field strength, only one signal is detected. Because of the spherical symmetry, the splitting pattern will be identical for all three canonical orientations, i.e., the spectra observed for H_X and H_Y applied fields will be identical to the spectrum observed for H_Z.

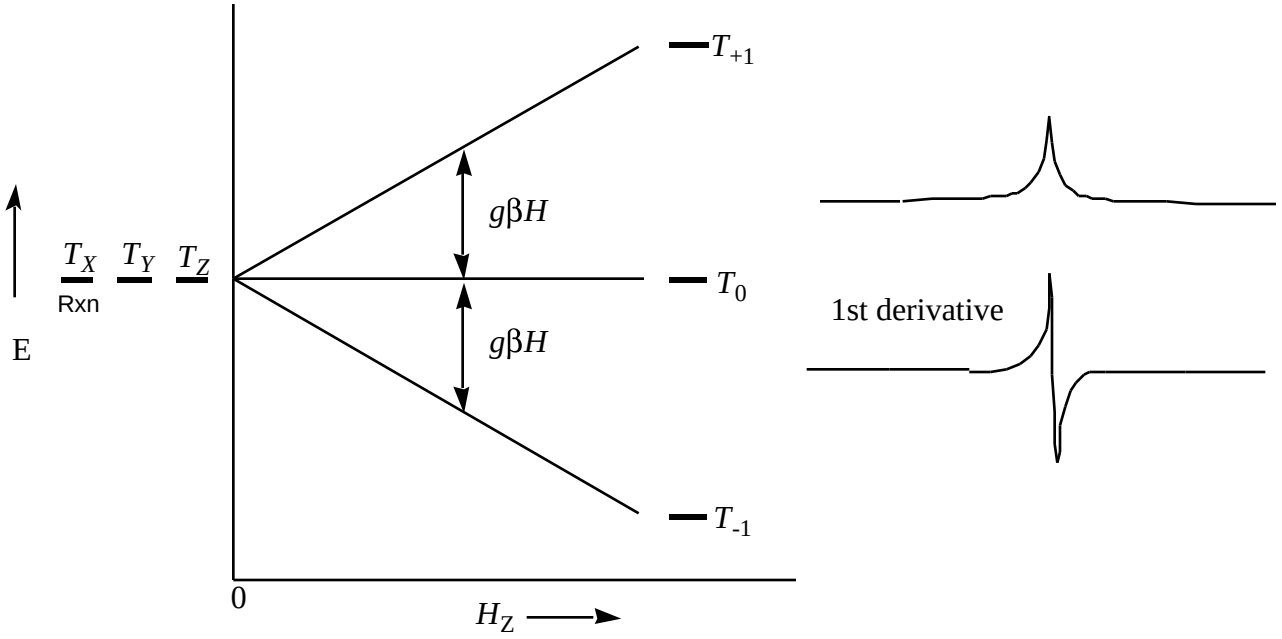

Figure IX.6. Energy diagram and absorption curves for $S = 1$ cubic system.

Lowering the symmetry from cubic symmetry to axial and rhombic symmetries results in energy splittings similar to those depicted in Figures IX.7 and IX.8, respectively. The solid arrows represent the $\Delta M_S = 1$ allowed transitions. The dotted arrow represents the $\Delta M_S = 2$ formally forbidden transition (*vide infra*).

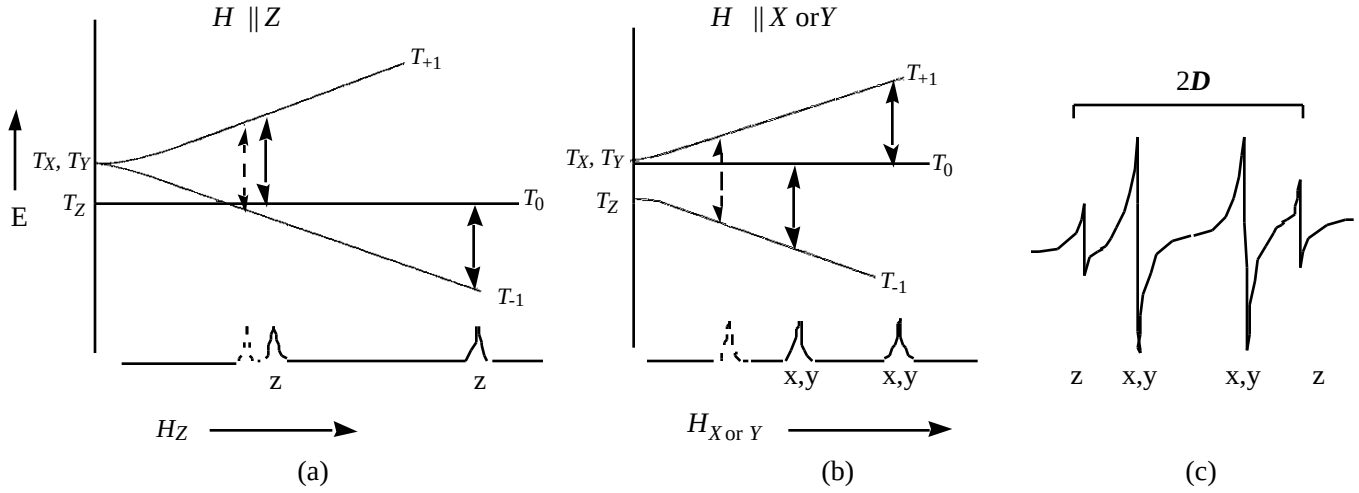

Figure IX.7. Energy diagram and absorption curves for $S = 1$ $\boldsymbol{D} > 0$ axial system. (a) Applied field aligned with the molecular Z-axis. (b) Applied field aligned with the molecular X- or Y-axis. (c) Simulated spectrum of absorptions.

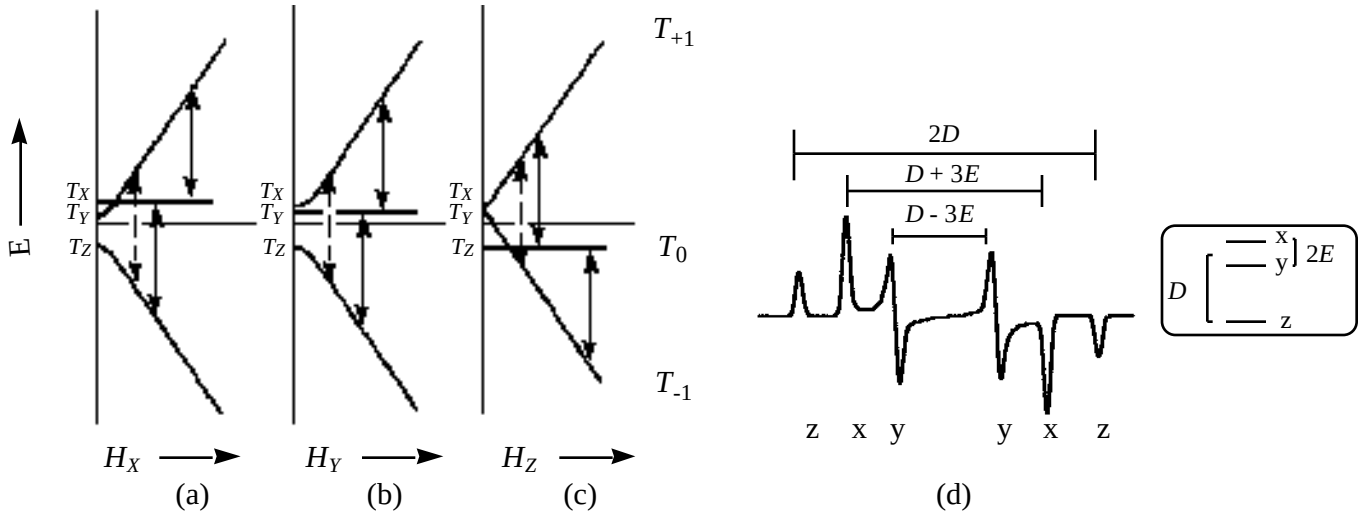

Figure IX.8. Energy diagram and absorption curves for $S = 1$, $\boldsymbol{D} > 0$ and $|\boldsymbol{D}| \neq 3|\boldsymbol{E}|$ rhombic system. (a) Applied field aligned with the molecular Z-axis. (b) Applied field aligned with the molecular Y-axis. (c) Applied field aligned with the molecular X-axis. (d) Simulated spectrum of absorptions and ZFS parameter determination.

As the strength of the applied field increases the major cause of the energy splittings shifts from the molecular quantization due to the spin-dipolar coupling (with eigenfunctions T_X, T_Y T_Z) to the applied field quantization described by the Zeeman effect (with eigenfunctions T_{+1}, T_0, T_{-1}.) The zero-field triplet eigenfunctions, T_X, T_Y T_Z, are not the same as the eigenfunctions of the high-field spin Hamiltonian, T_{+1}, T_0, T_{-1}. The zero-field eigenfunctions are rather a mixture of the high-field eigenfunctions.

$$\begin{aligned} T_X &= {}^{1}\!/\!_{\sqrt{2}}\,(T_{-1} - T_{+1}) \\ T_Y &= {}^{i}\!/\!_{\sqrt{2}}\,(T_{-1} + T_{+1}) \\ T_Z &= T_0 \end{aligned} \qquad (2)$$

The spin quantum numbers, $M_S = \pm 1,0$, are "good" quantum numbers for the high-field eigenfunctions, but not for the zero-field eigenfunctions. The dashed arrows in Figures IX.7 and IX.8 at low fields represent the $\Delta M_S = 2$ transition which is formally forbidden. At lower fields the spin quantum numbers, $M_S = \pm 1,0$, are not well-defined and thus the selection rule is relaxed.

Several important differences are noted between EPR spectra of cubic, axial and rhombic systems. Whereas the energy splitting pattern of a cubic system is the same regardless of the applied field orientation, the energy splitting pattern of an axial or rhombic system is dependent upon the orientation of the applied field. Therefore the $\Delta M_S = 1$ transitions for axial and rhombic systems do not occur at the same field strength as does the transitions for cubic systems. Two and three absorptions are observed for axial and

rhombic systems, respectively, for each canonical orientation instead of one. For an axial system two states remain degenerate at zero field (T_X and T_Y in Figure IX.7) and application of the fields H_X and H_Y will result in absorptions at the same field strength. The absorption due to the application of the unique field direction (H_Z), however, will occur at a different field strength as seen in Figure IX.7. Therefore an axially symmetric system is generally characterized by a four line spectrum with the distance between the outermost peaks equal to $2\boldsymbol{D}$ as shown in (c) of Figure IX.7. For a rhombic system with $|\boldsymbol{D}| \neq 3|\boldsymbol{E}|$ each canonical orientation will result in a different spectrum leading to a six line spectrum shown in (d) of Figure IX.8. From the spectrum it is possible to determine the energy values of $\boldsymbol{D}$ and $\boldsymbol{E}$ by the relations given in (d). When $|\boldsymbol{D}| = 3|\boldsymbol{E}|$ (refer to the peak labels in (d) of Figure IX.8) the two innermost peaks labeled "y" collapse to one central peak and the peaks labeled "x" coincide with the peaks labeled "z" resulting in a three line spectrum.

It may be helpful to examine the energy splittings at a fixed field strength while sweeping the frequency.[4] For simplicity we will assume $\boldsymbol{E} = 0$.

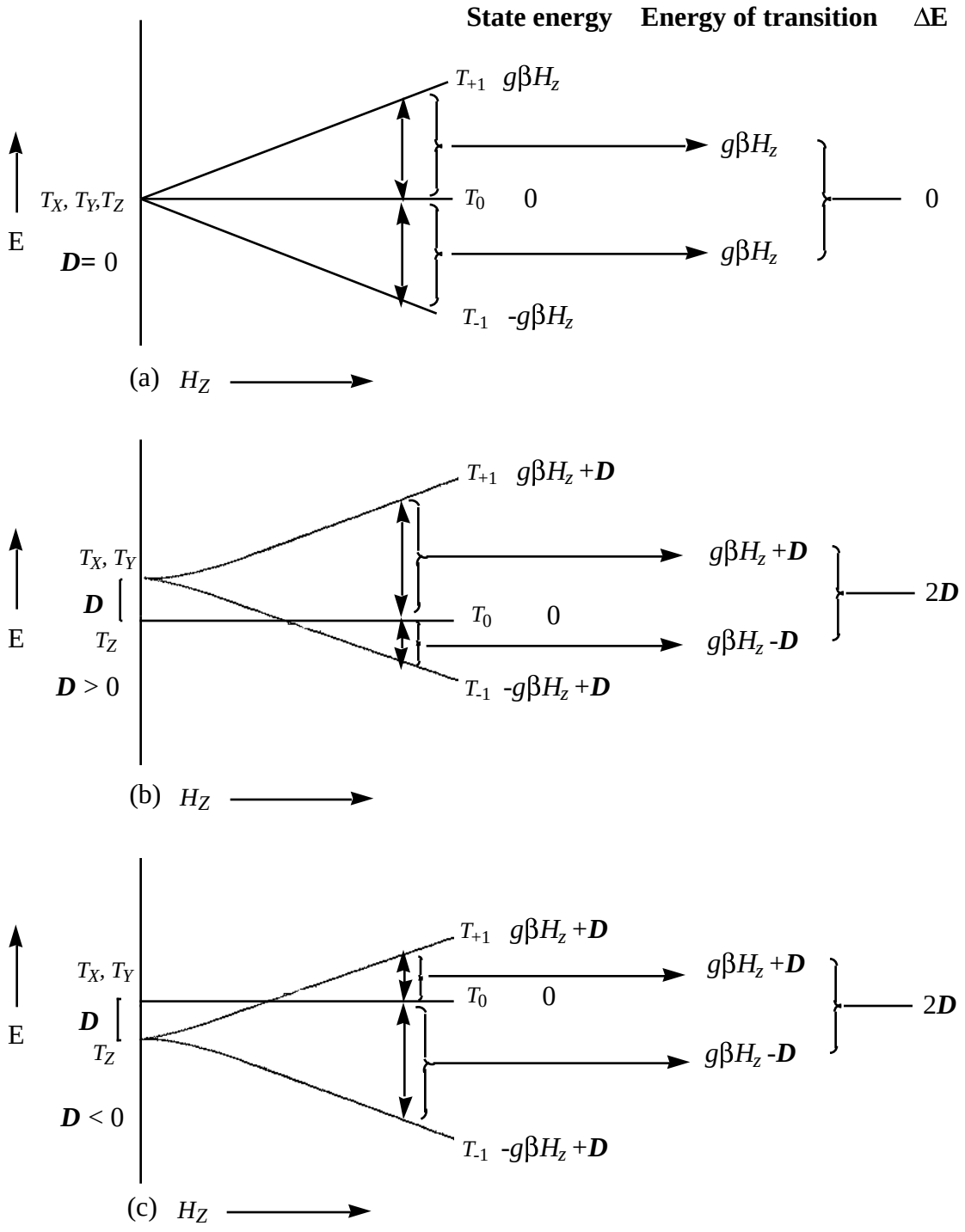

Figure IX.9. Energy levels of a triplet system. (a) Without dipolar interaction. (b) With dipolar interaction where $\boldsymbol{E} = 0$ and $\boldsymbol{D} > 0$. (c) With dipolar interaction where $\boldsymbol{E} = 0$ and $\boldsymbol{D} < 0$.

If the field is kept constant the difference in transition energy is equal to 2***D*** and if the transition energy is kept constant the difference in field strength is equal to 2***D***.

It should be noted that the spectra described in Figures IX.7 and IX.8 are not usually observed if the experiment is performed in solution at room temperature. As intimated earlier the two main contributors to

the effective magnetic field at one electron are the externally applied field (H_Z) and the internal field associated with the other electron described by

$$H_{eff} = H_Z + \frac{\mu_{eff}(3\cos^2\theta - 1)}{r^3} \tag{3}$$

where r is the distance between the unpaired electrons and θ is the angle formed by the applied field and the vector connecting the unpaired electrons.

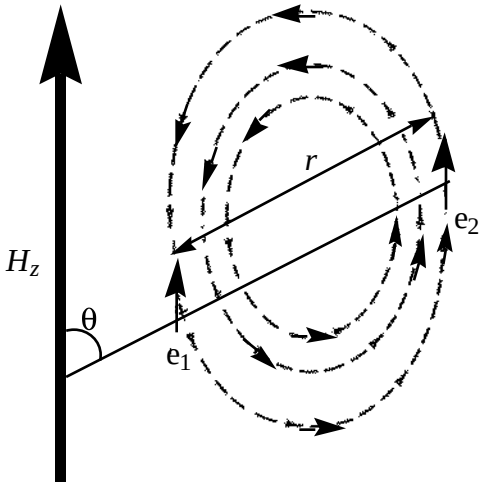

If the EPR experiment is performed in solution at room temperature the rapid tumbling on the time scale of the experiment causes the angular dependence term in equation 3 to average to zero and all spectroscopic consequences of dipolar coupling are eliminated. Therefore to observe manifestations of ZFS it is necessary to perform the experiment on powders or frozen glassy samples.

In summary, the ZFS parameters ***D*** and ***E*** provide valuable information about the electron distribution in high-spin systems and are used to interpret the solid or frozen EPR spectra of these systems. Turning our attention from the physical manifestations of the ZFS parameters, we now focus on the theoretical treatments of ***D*** and ***E***.

IX.4 Theoretical Treatment of the Zero Splitting Parameter *D*[1,2,4,7,8]

As mentioned earlier, the phenomenological Hamiltonian used to describe the spin-spin interaction energy is

$$\hat{H} = \hat{S} \cdot \mathbf{D} \cdot \hat{S} \tag{4}$$

where $\hat{S}$ is the total spin operator of the two electrons ($\hat{S} = \hat{S}_1 + \hat{S}_2$) and **D** is a symmetric, traceless tensor. Since the spin dipole-dipole interaction is anisotropic, it depends on the relative orientations of spins and thus requires a tensor to adequately describe its energy. The expanded form of equation 4 is

$$\hat{H} = \frac{g^2\beta^2}{2}\left[\hat{S}_X, \hat{S}_Y, \hat{S}_Z,\right] \begin{bmatrix} \frac{r^2 - 3x^2}{r^5} & \frac{-3xy}{r^5} & \frac{-3xz}{r^5} \\ \frac{-3yx}{r^5} & \frac{r^2 - 3y^2}{r^5} & \frac{-3yz}{r^5} \\ \frac{-3zx}{r^5} & \frac{-3zy}{r^5} & \frac{r^2 - 3z^2}{r^5} \end{bmatrix} \begin{bmatrix} \hat{S}_X \\ \hat{S}_Y \\ \hat{S}_Z \end{bmatrix} \quad (5)$$

where $\hat{S}_i$ is the component of the spin operator in the *i*-direction (*i* = *x*, *y* or *z*), *r* is the interelectronic distance and *x*, *y* or *z* are the respective components of the interelectronic distance in Cartesian coordinates. If the system is rotated so that the principle axis system of the dipolar interaction is parallel with the molecular axis system, the off diagonal elements become zero and the **D** tensor is said to be diagonalized. In this principle axis frame equation 5 can be rewritten as,

$$H = D_{XX}S_X^2 + D_{YY}S_Y^2 + D_{ZZ}S_Z^2 \quad (6)$$

where D_{XX}, D_{YY}, and D_{ZZ} are the principle values of the tensor whose negatives are the zero field energies of the three sublevels of the triplet state. If the *Z*-axis lies along the symmetry axis perpendicular to the plane of the molecule and the *X*-axis coincides with one of the other symmetry axes (if one exists) expressions for ***D*** and ***E*** are

$$\boldsymbol{D} = \tfrac{3}{2} D_{ZZ} \quad (7)$$

$$\boldsymbol{E} = \tfrac{1}{2}\left|D_{XX} - D_{YY}\right| \quad (8)$$

When the tensor elements of equation 5 are averaged over the electronic wavefunction and the tensor diagonalized, the expressions for ***D*** and ***E*** take the form

$$\boldsymbol{D} = \tfrac{3}{2}\left(\frac{g^2\beta^2}{2}\right)\left\langle \frac{r^2 - 3z^2}{r^5} \right\rangle = \frac{3}{4} g^2\beta^2 \left\langle \frac{r^2 - 3z^2}{r^5} \right\rangle \quad (9)$$

$$\boldsymbol{E} = \tfrac{1}{2}\left(\frac{g^2\beta^2}{2}\right)\left|\left\langle \frac{r^2 - 3x^2}{r^5} - \frac{r^2 - 3y^2}{r^5} \right\rangle\right| = \frac{3}{4} g^2\beta^2 \left|\left\langle \frac{y^2 - x^2}{r^5} \right\rangle\right| \quad (10)$$

From these two parameters the zero field energy level splittings can be adequately described (in the absence of spin-orbit coupling). ***D*** measures the average distance between the two electrons and is inversely proportional to the cube of that distance (***D*** r^{-3}) while ***E*** describes the deviation of the electron distribution from axial symmetry. (***D*** has been referred to as the axial ZFS parameter and ***E*** as the rhombic parameter.[7])

To rigorously calculate ***D*** and ***E*** requires the use high level *ab initio* derived wavefunctions. Rigorous theoretical determinations of ***D*** using high-quality *ab initio* wave functions have been performed for the excited triplet states of formaldehyde,[9] benzene and naphthalene[10] and ground state triplet states for methylene[11] and trimethylenemethane.[12] Although it is theoretically possible to determine ***D*** with *ab initio* basis sets and electron correlation, it may not be computationally practical which has led to the derivation of approximate methods to simplify the task of evaluating the large number of integrals involved for even moderate sized molecules.[2] These various approximations used for the theoretical determination of ***D*** have been presented in the literature over the last several decades.[10,13-27]

Most of these approximations are derived from the first-order perturbation expression for ***D*** given in equation 11 treating only the spin-spin interaction. $\psi(1,2)$ is the antisymmetric orbital wave function (necessary for the triplet state) which can be written using the molecular orbitals that contain the unpaired electrons, φ_i and φ_j .

$$D = \tfrac{3}{2} g^2 \beta^2 \langle \psi(1,2) | D_{op} | \psi(1,2) \rangle \tag{11}$$

$$\psi(1,2) = \tfrac{1}{\sqrt{2}} \{ \varphi_i(1)\varphi_j(2) - \varphi_j(1)\varphi_i(2) \} \tag{12}$$

D_{op} is the dipole-dipole operator[21]

$$D_{op} = \frac{r_{12}^2 - 3z_{12}^2}{r_{12}^5} \tag{13}$$

where the *Z*-axis is the molecular axis along which the spin-spin interaction is greatest. When φ_i is expressed as the LCAO-MO approximation

$$\varphi_i = \sum_i c_{ir} \chi_r \tag{14}$$

and only two-center Coulomb terms are considered, equation 11 becomes

$$D = \tfrac{3}{4} g^2 \beta^2 \sum_{p<q} (c_{ip}c_{jq} - c_{iq}c_{jp})^2 \langle pp | qq \rangle \tag{15}$$

where

$$\langle pp|qq \rangle = \left\langle \chi_p(1)\chi_p(1) \left| \frac{r_{12}^2 - 3z_{12}^2}{r_{12}^5} \right| \chi_q(2)\chi_q(2) \right\rangle . \tag{16}$$

An approximation for $\langle pp|qq \rangle$ which is frequently used to simplify the integral calculations is the point-dipole approximation[21] given in equation 17

$$\frac{1}{2}\left(\frac{1}{r^3}+\frac{r^2-2d^2}{\left(r^2+d^2\right)^{5/2}}\right) \tag{17}$$

where r is distance between the atomic centers p and q and d is the vertical distance between half-charges located above and below the molecular plane (taken as the representing the p_z orbital of carbon.) Reasonable results have been obtained when d = 1.4 Å. Further modifications of the point-dipole approximation which have been used include[21]

$$\frac{1}{\left(r^2+d^2\right)^{3/2}} \tag{18}$$

$$\frac{1}{2}\left[\frac{1}{r^3}+\frac{1}{\left(r^2+1.96\right)^{3/2}}\right]. \tag{19}$$

An approximation for the $\left(c_{ip}c_{jq}-c_{iq}c_{jp}\right)^2$ term has also been presented[21] and reduces to $\rho_p\rho_q$ where $\rho_p = c_{ip}^2 + c_{jp}^2$. Another approximation, which is frequently used by Mukai, is shown in equation 20 where r_{ij} is the distance between atoms i and j, m_{ij} is the distance vector along the axis which gives rise to the largest dipole-dipole interaction, and ρ_i and ρ_j are the spin densities on atoms i and j.[13,25]

$$D = \tfrac{3}{4}g^2\beta^2\sum_{i,j}\frac{r_{ij}^2-3m_{ij}^2}{r_{ij}^5}\rho_i\rho_j \tag{20}$$

This equation has been used to give reasonable ***D***-value approximations for biradicals with localized electron distributions that can be separated into monoradical halves with atoms i and j belonging to different halves (hereafter referred to as localized biradicals.) The spin densities used are those of each monoradical half. It has been noted that this equation provides only crude approximations for delocalized biradicals[27] which initiated an investigation in our lab into finding an approximation method that would provide more reasonable ***D***-values for delocalized biradicals due to our interest in nondisjoint organic molecules with $S > 1/2$.[28] The problem we encountered in trying to use equation 20 for delocalized radical systems was that the delocalized system could not be separated into monoradical halves due to shared spin-containing atoms (hereafter referred to as delocalized biradicals). Since the dipole-dipole interaction, and thus the ***D***-value, strongly depend on the average distance between the two unpaired electrons (varying as $1/r^3$),[29] the question

is, how does one determine the "average" distance? With this in mind, we found a phenomenological method with which we have been able to calculate reasonable ***D***-values for delocalized biradicals.

References

1) Atherton, N. M. *Principles of Electron Spin Resonance*; Ellis Horwood PTR Prentice Hall: New York, 1993.
2) Berson, J. A. *The Chemistry of the Quinonoid Compounds, Vol. II*; Patai, S. R., Z., Ed.; John Wiley & Sons: New York, 1988, pp 482.
3) Hanna, M. *Quantum Mechanics in Chemistry*; Hanna, M. Quantum Mechanics in Chemistry; The Benjamin/Cummings Publishing Company, Inc.: Menlo Park, CA, 1981: Menlo Park, CA, 1981.
4) Bersohn, M.; Baird, J. C. *An Introduction to Electron Paramagnetic Resonance*; W. A. Benjamin, Inc.: New York, 1966.
5) El-Sayed, M. A. *Pure Appl. Chem.* **1970**, *24*, 475-493.
6) Angiolillo, P. J.; Lin, V. S.-Y.; Vanderkooi, J. M.; Therien, M. J. *J. Am. Chem. Soc.* **1995**, *117*, 12514-12527.
7) Kahn, O. *Molecular Magnetism*; VCH: New York, 1993.
8) Wertz, J. E.; Bolton, J. R. *Electron Spin Resonance*; Chapman and Hall: New York, 1986.
9) Langhoff, S. R.; Elbert, S. T.; Davidson, E. R. *Int. J. Quantum Chem.* **1973**, *7*, 999-1019.
10) Godfrey, M.; Kern, C. W.; Karplus, M. *J. Chem. Phys.* **1966**, *44*, 4459-4469.
11) Langhoff, S. R.; Elbert, S. T.; Davidson, E. R. *Int. J. Quantum Chem.* **1973**, *7*, 759-777.
12) Feller, D.; Borden, W. T.; Davidson, E. R. *J. Chem. Phys.* **1981**, *74*, 2256-2259.
13) Mukai, K.; Tamaki, T. *Bull. Chem. Soc. Jpn.* **1977**, *50*, 1239-1244.
14) Tinkham, M.; Strandberg, M. W. P. *Phys. Rev.* **1955**, *97*, 937-951.
15) McWeeny, R. *J. Chem. Phys.* **1961**, *34*, 399-401.
16) McLachlan, A. D. *Mol. Phys.* **1962**, *5*, 51-62.
17) Higuchi, J. *J. Chem. Phys.* **1963**, *38*, 1237-1245.
18) Van der Waals, J. H.; Ter Maten, G. *Mol. Phys.* **1964**, *8*, 301-318.
19) Shulman, R. G.; Rahn, R. O. *J. Chem. Phys.* **1966**, *45*, 2940-2946.
20) Wiersma, D. A.; Kommandeur, J. *Mol. Phys.* **1967**, *13*, 241-252.
21) Pullman, A.; Kochanski, E. *Int. J. Quantum Chem.* **1967**, *1S*, 251-259.
22) Calder, A.; Forrester, A. R.; James, P. G.; Luckhurst, G. R. *J. Am. Chem. Soc.* **1969**, *91*, 3724.
23) Luckhurst, G. R.; Pedulli, G. F. *J. Chem. Soc., B* **1971**, 329-334.
24) Azuma, N.; Ohya-Nishiguchi, H.; Yamauchi, J.; Mukai, K.; Deguchi, Y. *Bull. Chem. Soc. Jpn.* **1974**, *47*, 2369-2375.
25) Mukai, K.; Sakamoto, J. *J. Chem. Phys.* **1978**, *68*, 1432-1438.
26) Mukai, K.; Inagaki, N. *Bull. Chem. Soc. Jpn.* **1980**, *53*, 2695-2700.
27) Kirste, B.; Tian, P.; Kalisch, W.; Kurreck, H. *J. Chem. Soc. Perkin Trans. 2* **1995**, 2147-2152.
28) Shultz, D. A.; Boal, A. K.; Farmer, G. T. *J. Am. Chem. Soc.* **1997**, *119*, 3846.
29) Jain, R.; Sponsler, M. B.; Coms, F. D.; Dougherty, D. A. *J. Am. Chem. Soc.* **1988**, *110*, 1356-1366.